

Original research article

## Dosimetric investigation of a new high dose rate $^{192}\text{Ir}$ brachytherapy source, IRAsource, by Monte Carlo method

Atefeh Rostami<sup>a</sup>, Mahdi Hoseini<sup>b</sup>, Mahdi Ghorbani<sup>c,\*</sup>, Courtney Knaup<sup>d</sup><sup>a</sup> Department of Medical Physics and Radiological Sciences, Faculty of Paramedical Sciences, Sabzevar University of Medical Sciences, Sabzevar, Iran<sup>b</sup> Department of Medical Physics, Faculty of Medicine, Mashhad University of Medical Sciences, Mashhad, Iran<sup>c</sup> Cancer Research Center, Shahid Beheshti University of Medical Sciences, Tehran, Iran<sup>d</sup> Comprehensive Cancer Centers of Nevada, Las Vegas, Nevada, USA

## ARTICLE INFO

## Article history:

Received 2 July 2019

Received in revised form

11 November 2019

Accepted 23 December 2019

Available online 26 December 2019

## Keywords:

Brachytherapy

Dosimetric parameters

IRAsource source

MCNPX

## ABSTRACT

**Purpose:** The purpose of the present study was to perform an independent calculation of dosimetric parameters associated with a new  $^{192}\text{Ir}$  brachytherapy source model, IRAsource.

**Materials and methods:** The parameters of air kerma strength (AKS), dose rate constant (DRC), geometry function (GF), radial dose function (RDF), as well as two-dimensional (2D) anisotropy function (AF) of IRAsource  $^{192}\text{Ir}$  source model were calculated in this study. The MC n-particle extended (MCNPX) code was also employed for simulating high dose rate (HDR), IRAsource and  $^{192}\text{Ir}$  source; and formalism was used for calculating dosimetry parameters based on task group number 43 updated report (TG-43 U1).

**Results:** The results of this study were consistent with the ones reported about the IRAsource source by Sarabiasl et al. The AKS per 1 mCi activity and the DRC values were also equal to  $3.65 \text{ cGy cm}^2 \text{ h}^{-1} \text{ mCi}^{-1}$  and  $1.094 \text{ cGy h}^{-1} \text{ U}^{-1}$ ; respectively. The comparison of the results of the DRC and the RDF reported by Sarabiasl et al. also validated the  $^{192}\text{Ir}$  IRAsource simulation in this study. Moreover, the AFs of IRAsource source model were in a good agreement with those of Sarabiasl et al. at different distances, which could be attributed to identical geometries.

**Conclusion:** In line with those reported by Sarabiasl et al., the results of this study confirmed the IRAsource  $^{192}\text{Ir}$  source for clinical uses. The calculated dosimetric parameters of the IRAsource source could be utilized in clinical practices as input data sets or for validation of treatment planning system calculations.

© 2020 Greater Poland Cancer Centre. Published by Elsevier B.V. All rights reserved.

### 1. Purpose

Radiation therapy, classified into teletherapy and brachytherapy, is taken into account as one major modality of cancer treatment. Due to high radiation dose directed at the tumor and low exposure of normal surrounding tissues; brachytherapy has been widely used, over the past two decades, for the treatment of different kinds of tumors such as prostate, breast, and cervix.<sup>1,2</sup>

It should be noted that determination of radiation absorbed dose in tumors and normal tissues surrounding radioactive implants in a precise manner is of paramount importance prior to brachytherapy.<sup>3</sup> Primary photons are thus absorbed by the source core and there is an anisotropic dose distribution around HDR  $^{192}\text{Ir}$  sources. Hence, a specific dataset is required for each source

before it can be used in clinical applications.<sup>3,4</sup> According to the recommendations made by the American Association of Physicists in Medicine (AAPM), Task Group No. 43 (TG-43); evaluation along with verification of dosimetric parameters of brachytherapy sources including AKS, DRC, RDF, AF are essential before their application in clinical practices.<sup>5</sup> Besides, the dosimetric parameters of brachytherapy sources can be investigated using MC and experimental methods.

There are various designs of HDR  $^{192}\text{Ir}$  brachytherapy sources that are different in shape and design of active parts or the capsule containing the sources. Some of after-loading systems used for HDR  $^{192}\text{Ir}$  brachytherapy include Flexisource,<sup>6</sup> Varisource,<sup>7</sup> M-19,<sup>8</sup> and BEBIG.<sup>9</sup> So far, the dosimetric parameters of different HDR  $^{192}\text{Ir}$  brachytherapy sources have been evaluated by MC methods using several MC codes such as MCNP, Penelope, and Geant4.<sup>6,9</sup> It has been also reported that the data can be extended to clinical uses for developing brachytherapy planning system programs.

Recently, a new HDR  $^{192}\text{Ir}$  brachytherapy source model; called IRAsource, has been introduced by Nuclear Science and Technology

This study was performed at Cancer Research Center (Shahid Beheshti University of Medical Sciences, Tehran, Iran)

\* Corresponding author.

E-mail address: [mhdghorbani@gmail.com](mailto:mhdghorbani@gmail.com) (M. Ghorbani).

Research Institute (NSTRI, Tehran, Iran) to be used in HDR after-loading brachytherapy.<sup>1</sup> Currently, IRAsource is in the preclinical stage and several independent experimental and simulation studies are needed to evaluate the dosimetry properties of this source model.

In a study by Sarabiasl et al.,<sup>10</sup> MCNP4C code was utilized for MC simulation of dose rate distributions around the HDR <sup>192</sup>Ir IRAsource source. As well, all of dosimetry parameters reported by the AAPM TG-43 were evaluated by Sarabiasl et al.<sup>10</sup> and the results were compared with other sources used for clinical applications. In the same vein, Ayoobian et al.<sup>11</sup> evaluated the 2D relative dose distribution around the IRAsource. The measurements were then performed by EBT and HD-810 Gafchromic films and radiochromic films in polymethylmethacrylate (PMMA) phantom on the basis of recommended AAPM reports, numbers 43 (TG-43) and 55 (TG-55). In the study by Ayoobian et al.,<sup>11</sup> the values of DRC, RDF and 2D AF were measured and calculated at radial distances of 0.5–4 cm. The data obtained from two MC and experimental studies undertaken by Sarabiasl et al.<sup>10</sup> as well as those in the investigation by Ayoobian et al.<sup>11</sup> were in a good agreement. Two studies by Sarabiasl et al.<sup>10</sup> and Ayoobian et al.<sup>11</sup> for the IRAsource are considered to be independent because the AAPM independence condition is not referred to authors but to studies. Although two independent theoretical (i.e., MC based) and experimental studies are adequate for the validation of a new source according to the AAPM report, but the results of different studies could be used to build a database like those presented in the imaging and radiation oncology core (IROC) webpage<sup>12</sup> or the Valencia University webpage<sup>13</sup> for collecting and reporting the findings of dosimetric parameters of diverse brachytherapy sources that are necessary for clinical application. On the other hand, in the study of Sarabiasl, et al. there is no mention of using the recommendations by the report of AAPM and ESTRO<sup>3</sup> for MC simulation of high energy sources that are used in the MC methodology of this study.

The purpose of the present study was to perform an independent calculation of dosimetric parameters of AKS, DRC, RDF, and AF around the first prototype of the HDR IRAsource <sup>192</sup>Ir brachytherapy source model, in vacuum and water phantoms, using MC code. The results of MC simulation could be then compared with similar HDR <sup>192</sup>Ir sources, commonly used in clinical contexts.

## 2. Materials and methods

### 2.1. Geometry of IRAsource <sup>192</sup>Ir brachytherapy source

The active core of the IRAsource source consists of pure and homogenous <sup>192</sup>Ir radionuclide with a density of 22.42 g/cm<sup>3</sup>. The length and the diameter of the active core are also 3.5 mm and 0.6 mm, respectively. The capsule is a 304 L stainless steel tube (with a density of 8.02 g/cm<sup>3</sup>), 4.63 mm in length and 0.9 mm in diameter. As well, the end of the tube is in the shape of a 304 L stainless steel hemisphere. The distance between the capsule tip and the pellet surface of the active core is equal to 0.53 mm. A woven 316 L stainless steel cable (0.86 mm and 4 mm in diameter and length, respectively) is similarly connected to the other side of the active core. It should be noted that the data for simulation of geometry

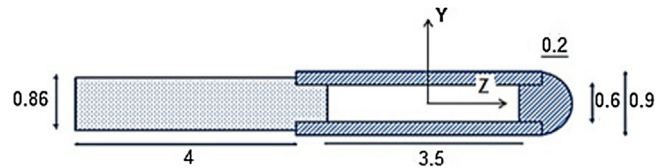


Fig. 1. Schematic description of the simulated geometry for the IRAsource <sup>192</sup>Ir source (the numbers are in mm).

and compositions of materials were derived from Sarabiasl et al.<sup>10</sup> A schematic description of the geometry used in this simulation was presented in Fig. 1, and an additional description of the geometry and its corresponding parameters were listed in Table 1.

### 2.2. Calculation of TG-43 dosimetric parameters

To calculate dosimetry, the source was initially defined at the center of a spherical phantom with a radius of 40 cm as described in the reference.<sup>10</sup> The spherical phantom radius for calculation of AKS was 50 cm. In the recent report by Task Group 43 of AAPM (TG-43 U1), parameters for dosimetry of brachytherapy sources were used in the simulation.<sup>14</sup> The details of the simulation including phantom size, tori thicknesses, as well as energy cut-off were based on the recommendations by the report of AAPM and ESTRO on dose calculation for high energy photon-emitting brachytherapy sources.<sup>3</sup>

Likewise, the MCNPX code (version 2.6.0) was employed to simulate HDR <sup>192</sup>Ir IRAsource source and, subsequently, formalism was employed for calculation of dosimetry parameters based on TG-43 U1 protocol. The energy spectrum of the <sup>192</sup>Ir source taken from the National Nuclear Data Center database<sup>15</sup> was presented in Table 2.

In all simulation programs, the energy cut-off was set at 10 keV. As recommended in the TG-43 U1 report, air and water were, respectively, considered with densities of 0.0012 g/cm<sup>3</sup> (humidity of 40%) and 0.998 g/cm<sup>3</sup> (22 °). Further details about the materials used in this study were outlined in Table 3. The details regarding simulation and calculation of each dosimetry parameter were explained as follows.

### 2.3. Air kerma strength

In order to estimate the AKS for the <sup>192</sup>Ir IRAsource source, several tori were initially defined at various radial distances (from 1 to 39 cm) in a 50-cm radius spherical volume. The AKS was then computed in a transversal axis of the source by tori cells using F6 tally. The thicknesses of the tori varied in relation to the axial distance of the tori from the center of the source (Table 4).<sup>16</sup> The space within the tally volume was considered as air and that outside tori volume was assumed as vacuum for the calculation of AKS. Finally, the output of air kerma program was multiplied by the squares of radial distance (air kerma rate  $\times d^2$ ) to compute  $S_k$ , and then plotted based on the radial distance. The plot had a relatively flat portion and the average value of air kerma was used for AKS calculation.

Table 1  
Further details of the <sup>192</sup>Ir IRAsource geometry.

Component	Inside diameter (mm)	Outside diameter (mm)	Length (mm)	Density (g/cm <sup>3</sup> )	Remarks
Iridium metal	–	0.6	3.5	22.42	Active element
Encapsulation	0.9	0.6	4.63	8.02	Stainless steel; 0.53 mm thick, Hemispherical welded end
Cable	–	0.86	4	8.02	Stainless steel

**Table 2**  
Energy spectrum of the  $^{192}\text{Ir}$  source.

Energy (keV)	Intensity (%)
9.44	3.92
65.12	2.62
66.83	4.44
75.36	0.531
75.74	1.021
77.83	0.364
136.39	0.199
176.98	0.004
280.27	0.008
295.95	28.71
308.45	29.70
316.50	82.86
416.46	0.670
468.06	47.84
485	0.004
588.58	4.522
593.63	0.042
599.41	0.003
604.41	8.216
612.46	5.34
765.8	0.001
844.53	0.292
1061.49	0.053
1089.96	0.001
1378.50	0.001

**Table 3**  
Details of materials used in the geometry of IRASource.

Material	Composition (%)	Density (g/cm <sup>3</sup> )
Air	H: 0.0732	0.0012
	C: 0.0123	
	N: 75.0325	
	O: 23.6077	
	Ar: 1.2743	
Water	H: 11.1	0.998
	O: 88.9	
Source (active core)	Ir: 100	22.42
Stainless steel (304 L)	Cr: 19.04	8.02
	Fe: 71.82	
	Ni: 8.32	
	Cu: 0.22	
	Mo: 0.62	
Stainless steel (316 L)	Cr: 17.21	8.02
	Fe: 69.77	
	Ni: 10.17	
	Cu: 0.36	
	Mo: 2.52	

**Table 4**  
The thicknesses of tori based on the axial distance of the tori from the center of source.<sup>3</sup>

Thicknesses of the tori	Axial distances
0.1 mm	$r_{\text{source}} < r \leq 1 \text{ cm}$
0.5 mm	$1 < r \leq 5 \text{ cm}$
1 mm	$5 < r \leq 10 \text{ cm}$
2 mm	$10 < r \leq 20 \text{ cm and more}$

#### 2.4. Dose rate constant

To compute the DRC, the dose rate was scored by \*F8 tally in a 0.1-cm thick torus, defined at a distance of 1 cm from the source center in water phantom ( $\rho = 0.998 \text{ g/cm}^3$ ) with a radius of 40 cm. The space outside the water phantom up to a radius of 200 cm was considered as dry air. After scoring the tally, the output of \*F8 tally was divided by the mass of torus in the output file, and then DRC was computed through dividing the dose rate value at a distance of 1 cm by the AKS.

#### 2.5. Radial dose function

The RDF was calculated in tori cells, placed at various distances ranging from 1.0 to 15.0 cm along the transverse axis of the source. The tori were defined in a water phantom with a radius of 40 cm. Similar to the DRC program, the space up to a radius of 200 cm was considered as dry air; beyond the water phantom. The thickness of the tori was then determined based on the report by Taylor et al.<sup>16</sup> The outputs of \*F8 tally were also divided by the masses of tori and then the RDF was computed by a specific formula in accordance with the TG-43 U1 report. To obtain the geometric function at various distances, the linear source approximation was used; and then an active length of 3.5 mm was considered for all calculations.

To verify the  $^{192}\text{Ir}$  IRASource source simulation, the DRC and the RDF parameters were calculated for this source and, consequently, compared with those reported by Sarabiasl et al.<sup>10</sup> for the same source model.

#### 2.6. Anisotropy function

The 2D AF was calculated using linear source approximation at various distances ranging from 0.25 to 10 cm at 24 polar angles (ranging from 0° to 180°) inside a spherical water phantom, with a radius of 40 cm. The tori, overlapping with the source or the source cable, were also excluded from the given calculations. To lessen uncertainty, different tallies were utilized; depending on their distance from the source. For distances less than 1 cm and for those greater than 1 cm, F6 tally and \*F8 tally were considered; respectively.

Finally, the TG-43 dosimetric parameters of the  $^{192}\text{Ir}$  IRASource source were compared with the ones reported by Sarabiasl et al.<sup>10</sup> and other types of  $^{192}\text{Ir}$  brachytherapy sources (Flexisource,<sup>6</sup> BEBIG,<sup>9</sup> M19,<sup>8</sup> Varisource VS2000<sup>7</sup>) used by other researchers.

### 3. Results

#### 3.1. Uncertainty analysis

According to the recommendations of TG-43 and the National Institute of Standards and Technology (NIST) Technical Note No. 1297,<sup>17</sup> statistical uncertainties (type A) were extracted from the output files and systematic uncertainties (type B) were classified into volume averaging, energy spectrum, geometric dimensions of source and capsule, phantom cross-section ( $\mu/\rho$ ), and MC transport code. The sources of uncertainties were described as follows:

- Volume averaging: It was not taken into consideration due to its negligible value.<sup>18</sup>
- Energy spectrum: It was taken to be 0.5% for the  $^{192}\text{Ir}$  source.<sup>8</sup>
- Geometric design of the source: The maximum tolerance of source dimensions was 0.2% that induced 0.75% uncertainty in dose calculation.<sup>10</sup>
- Phantom cross-section ( $\mu/\rho$ ): It had an uncertainty of about 0.1% for the  $^{192}\text{Ir}$  source.<sup>19</sup>
- Monte Carlo transport code: Dosimetric variation caused by MC transport code was estimated at 0.05% by Rivard et al.<sup>20</sup>

Based on the root of quadratic summation of systematic uncertainties, the quadratic summation of systematic uncertainties was 0.83% and the combined type B uncertainty was equal to 0.91%. The combined uncertainty was also calculated for all dosimetric parameters, using quadratic summation of type A and type B uncertainties.

**Table 5**  
Dose rate constant ( $\text{cGy h}^{-1} \text{U}^{-1}$ ) of this paper and other studies for HDR  $^{192}\text{Ir}$  brachytherapy sources (IRAsource, Flexisource,<sup>6</sup> BEBIG,<sup>9</sup> M19,<sup>8</sup> and Varisource VS2000<sup>7</sup>).

Source model	IRAsource Our study	IRAsource <sup>10</sup>	Flexisource <sup>6</sup>	BEBIG <sup>9</sup>	VariSource VS2000 <sup>7</sup>	M-19 <sup>8</sup>
DRC ( $\text{cGy h}^{-1} \text{U}^{-1}$ )	1.094	1.112	1.109	1.108	1.035	1.13

**Table 6**  
Radial dose function of this study and other researches in HDR  $^{192}\text{Ir}$  brachytherapy sources (IRAsource, Flexisource,<sup>6</sup> BEBIG,<sup>9</sup> M19<sup>8</sup> and Varisource VS2000<sup>7</sup>).

Distance (cm)	Source models					
	IRAsource (This study)	IRAsource <sup>10</sup>	Flexisource <sup>6</sup>	BEBIG <sup>9</sup>	VariSource VS2000 <sup>7</sup>	M-19 <sup>8</sup>
0.1	0.976 ± 0/001	–	–	–	–	–
0.2	0.98 ± 0/001	–	–	–	–	–
0.3	0.982 ± 0.000	0.992	–	–	0.976	–
0.4	0.987 ± 0.002	0.995	–	–	0.989	–
0.5	0.989 ± 0.002	0.996	0.9965	0.9964	0.991	0.995
0.6	0.992 ± 0.001	0.997	–	–	–	–
0.7	0.997 ± 0.000	0.997	0.9983	0.9984	1.000	–
0.8	0.998 ± 0.003	0.998	–	–	–	–
0.9	0.999 ± 0.003	0.999	–	–	–	–
1.0	1 ± 0.008	1.000	1.0000	1.0000	1.000	1.000
1.5	1.006 ± 0.005	1.003	1.0017	1.0025	1.002	1.004
2.0	0.999 ± 0.003	1.005	1.0037	1.0035	1.006	1.008
2.5	0.996 ± 0.002	1.005	–	–	1.007	1.007
3.0	0.996 ± 0.002	1.006	1.0051	1.0052	1.005	1.009
4.0	0.995 ± 0.005	1.005	1.0034	1.0035	1.006	1.008
5.0	0.993 ± 0.006	1.002	0.9987	0.9990	0.995	1.005
6.0	0.988 ± 0.004	0.995	0.9912	0.9915	0.984	0.997
7.0	0.976 ± 0.001	0.985	0.9807	0.9814	–	0.998
8.0	0.975 ± 0.003	0.972	0.9680	0.9682	0.941	0.974
9.0	0.955 ± 0.001	0.959	–	–	–	0.958
10.0	0.931 ± 0.001	0.939	0.9349	0.9352	0.879	0.940
11.0	0.902 ± 0.003	–	–	–	–	–
12.0	0.881 ± 0.002	–	0.8937	0.8944	0.803	–
13.0	0.864 ± 0.002	–	–	–	–	–
14.0	0.834 ± 0.001	–	–	–	0.693	–
15.0	0.812 ± 0.001	–	0.8212	0.8214	0.604	–

The maximum type A uncertainty for the AKS was 0.2%, with a total error of 0.93%. For the DRC, the uncertainty of the output file of the program was estimated to be 3.5%, with a total error of 3.62%.

Considering the RDF, the total error was reported in Table 6 with a coverage factor of 3 ( $k = 3$ ). The maximum uncertainty (0.8%) was also at the distance of 1 cm from the source center. The total error for the AF was 5.49% for the radial distance of 1 cm and the degree of 5°. The total error of the AF at the distances of 0.5, 1, 5, and 10 cm were illustrated in Fig. 3 using  $k = 3$ .

### 3.2. Air kerma strength and dose rate constant

Considering the  $^{192}\text{Ir}$  IRAsource source, the AKS value per 1 mCi activity and DRC were  $3.65 \text{ cGy cm}^2 \text{ h}^{-1} \text{ mCi}^{-1}$  and  $1.09 \text{ cGy h}^{-1} \text{U}^{-1}$ ; respectively.

The DRC for various commercially available HDR  $^{192}\text{Ir}$  brachytherapy sources was listed in Table 5. The maximum MC uncertainty (type A) for the AKS and the DRC was equal to 0% and 3.15%, respectively.

### 3.3. Radial dose function

The RDF values for the  $^{192}\text{Ir}$  IRAsource source derived from the present study and those reported by Sarabiasl et al.<sup>10</sup> along with other models of  $^{192}\text{Ir}$  brachytherapy sources were presented in Table 6. The differences between the RDF results in this study and the data reported by Sarabiasl et al. were presented in Table 7. As can be seen, the largest difference was 1.04% (Table 7). The blank cells in Table 6 also represented points lacking any equivalent value

**Table 7**  
Percentage difference in radial dose function values of the present study and that of Sarabiasl et al.<sup>10</sup>

Distance (cm)	Difference (%)
0.3	–1.04
0.4	–0.84
0.5	–0.74
0.6	–0.50
0.7	0.00
0.8	–0.03
0.9	–0.23
1.0	0.00
1.5	–0.23
2.0	–0.63
2.5	–0.89
3.0	–1.00
4.0	–0.99
5.0	–0.90
6.0	–0.70
7.0	–0.98
8.0	–0.21
9.0	–0.41
10.0	–0.85

in other studies; therefore, they were excluded from this comparison. The largest uncertainty in RDF calculation was equal to 0.8%. Comparing the results in the present study with those reported by Sarabiasl et al. verified  $^{192}\text{Ir}$  IRAsource source simulation performed in this investigation. For a schematic comparison, the values of RDF from the present study and Sarabiasl et al.'s investigation for the IRAsource source were shown in Fig. 2.

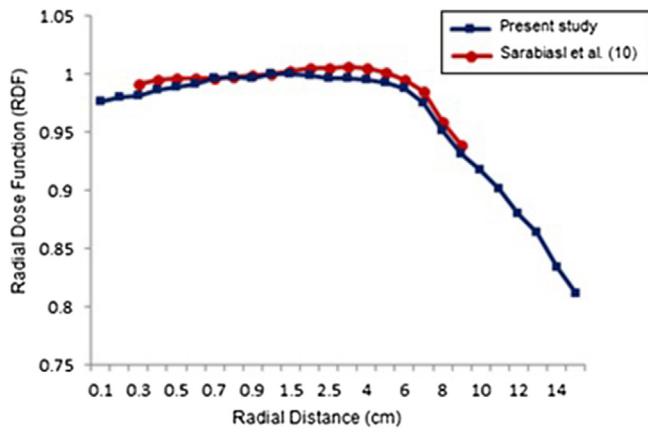


Fig. 2. Radial dose function for the IRAsource source from this study and Sarabiasl et al. study.<sup>10</sup>

### 3.4. Anisotropy function

The AF data for the IRAsource source at the distances of 0.5–10 cm and the angles of 0°–180° were illustrated in Table 8. To make a comparison of the AF values of the IRAsource source derived from this study and those reported by Sarabiasl et al., the corresponding diagrams at four distances of 0.5, 1, 5, and 10 cm were plotted in Fig. 3. The largest MC uncertainty (type A) in the AF calculation was equal to 2.05%.

## 4. Discussion

In this study, the dosimetry parameters of a new HDR <sup>192</sup>Ir brachytherapy source, i.e. the IRAsource model, were calculated, in compliance with TG-43 U1 recommendations, using MC simulation and then the results were presented in graphical and tabular forms. The findings were consistent with those reported in other studies on the designs of various <sup>192</sup>Ir sources, confirming their applications in clinical contexts.<sup>6,21,22</sup>

All the parameters of TG-43 report including AKS, DRC, RDF, and AF were calculated. To validate the accuracy of the simulation

data for this source, the parameters were compared with the ones reported by Sarabiasl et al.<sup>10</sup> The discussion was made in two parts. First, a comparison was drawn between the results of this study and those presented by Sarabiasl et al. for the <sup>192</sup>Ir IRAsource, and then the dosimetric parameters of <sup>192</sup>Ir IRAsource source model were compared with several <sup>192</sup>Ir source models, conventionally used in clinical contexts.

The DRC of the <sup>192</sup>Ir IRAsource source reported by Sarabiasl et al. was 1.62% higher than the DRC value obtained in the present study. With regard to similar geometries of IRAsource source model, this difference was within the acceptable range as it could be attributed to different codes used in both studies. In the study by Sarabiasl et al., simulations had been conducted via MCNP4C version of the code but the MCNPX code (version 2.6.0) was used in the present study for all simulation programs. The geometric parameters were also considered as important factors while comparing the results with other source models.

The difference between the DRC values of various <sup>192</sup>Ir brachytherapy source models, as reported in Table 5, was induced by the disparity of geometric parameters. Comparing the DRC values in different models, it became clear that the models with higher DRC but identical AKS could produce higher dose rates at the reference distance (1 cm) from the source in a water phantom. Based on the DRC values in different models, the dose rate of IRAsource at the reference distance was acceptable for clinical applications of brachytherapy. In the experimental study of IRAsource model undertaken by Ayoobian et al., the DRC values of 1.084 and 1.129 were obtained by EBT and HD-810 Gafchromic films and radiochromic films with a percentage difference of 0.922% and 3.1%; respectively.

The mean difference between the RDF values obtained in the present study, which were obtained for more radial distances (up to 15 cm), compared to the study by Sarabiasl et al., and those reported by Sarabiasl et al. was equal to 0.6%, which was in an acceptable range and also verified the simulation program adopted in this study. On the other hand, the maximum disagreement between the results of this study and those of the experimental research of IRAsource model carried out by Ayoobian et al. was 2.4%. A comparison of the RDF of IRAsource with other HDR <sup>192</sup>Ir sources was given in Table 6. To compare the RDF values of different sources,

Table 8  
Anisotropy function of the IRAsource source at distances of 0.5 cm–10 cm and angles of 0° to 180°.

θ (degrees)	Radial distance (cm)																	
	0.25	0.5	0.6	0.7	0.8	0.9	1.0	1.5	2.0	2.5	3.0	4.0	5.0	6.0	7.0	8.0	9.0	10.0
0	–	0.406	0.442	0.465	0.452	0.482	0.488	0.492	0.522	0.551	0.592	0.671	0.662	0.717	0.739	0.680	0.764	0.776
5	0.233	0.410	0.448	0.464	0.501	0.573	0.556	0.591	0.613	0.579	0.607	0.644	0.655	0.677	0.725	0.743	0.781	0.790
10	0.270	0.492	0.523	0.558	0.589	0.635	0.582	0.652	0.644	0.687	0.718	0.676	0.710	0.741	0.716	0.733	0.748	0.759
15	0.347	0.610	0.590	0.683	0.662	0.671	0.695	0.697	0.708	0.750	0.774	0.736	0.784	0.782	0.796	0.770	0.785	0.794
20	0.410	0.661	0.687	0.714	0.778	0.732	0.750	0.829	0.787	0.825	0.801	0.792	0.786	0.798	0.809	0.818	0.826	0.832
30	0.562	0.757	0.813	0.807	0.835	0.844	0.811	0.894	0.864	0.888	0.858	0.888	0.893	0.899	0.909	0.860	0.866	0.867
40	0.659	0.810	0.834	0.849	0.858	0.865	0.870	0.882	0.888	0.893	0.897	0.899	0.905	0.909	0.913	0.915	0.920	0.919
50	0.777	0.881	0.897	0.907	0.913	0.918	0.920	0.931	0.935	0.937	0.940	0.940	0.945	0.945	0.946	0.948	0.949	0.952
60	0.871	0.929	0.940	0.947	0.952	0.955	0.957	0.961	0.964	0.964	0.966	0.967	0.967	0.969	0.969	0.971	0.972	0.972
70	0.940	0.966	0.969	0.971	0.973	0.975	0.977	0.979	0.980	0.981	0.981	0.981	0.982	0.982	0.983	0.985	0.984	0.987
80	0.983	0.989	0.991	0.992	0.991	0.992	0.992	0.992	0.992	0.993	0.994	0.994	0.995	0.995	0.993	0.995	0.994	0.994
90	1.000	1.000	1.000	1.000	1.000	1.000	1.000	1.000	1.000	1.000	1.000	1.000	1.000	1.000	1.000	1.000	1.000	1.000
100	0.991	0.998	1.000	0.999	0.997	0.998	0.997	0.999	1.000	1.000	1.002	0.999	0.999	1.000	1.001	1.001	1.001	1.000
110	0.955	0.982	0.987	0.991	0.992	0.994	0.994	0.996	0.998	0.997	0.998	0.998	0.998	0.998	0.998	0.997	0.999	0.999
120	0.897	0.960	0.971	0.978	0.982	0.985	0.986	0.990	0.992	0.993	0.994	0.993	0.994	0.993	0.994	0.994	0.995	0.993
130	0.817	0.922	0.940	0.950	0.957	0.963	0.966	0.976	0.962	0.980	0.982	0.981	0.983	0.984	0.983	0.985	0.985	0.987
140	0.720	0.881	0.906	0.921	0.930	0.937	0.942	0.956	0.978	0.963	0.965	0.966	0.969	0.969	0.969	0.971	0.971	0.974
150	0.610	0.832	0.821	0.847	0.893	0.902	0.908	0.924	0.932	0.936	0.939	0.941	0.944	0.946	0.948	0.950	0.952	0.954
160	0.451	0.709	0.747	0.715	0.766	0.820	0.795	0.798	0.855	0.810	0.842	0.862	0.860	0.823	0.895	0.839	0.893	0.899
165	0.356	0.655	0.678	0.657	0.713	0.710	0.699	0.713	0.715	0.732	0.799	0.810	0.807	0.847	0.817	0.853	0.865	0.869
170	–	0.519	0.585	0.554	0.596	0.653	0.631	0.674	0.707	0.642	0.724	0.733	0.728	0.757	0.780	0.765	0.819	0.835
175	–	–	0.469	0.524	0.511	0.560	0.585	0.556	0.596	0.633	0.671	0.706	0.665	0.738	0.754	0.767	0.777	0.788
180	–	–	0.454	0.491	0.502	0.522	0.473	0.517	0.541	0.564	0.582	0.612	0.637	0.667	0.683	0.706	0.722	0.732

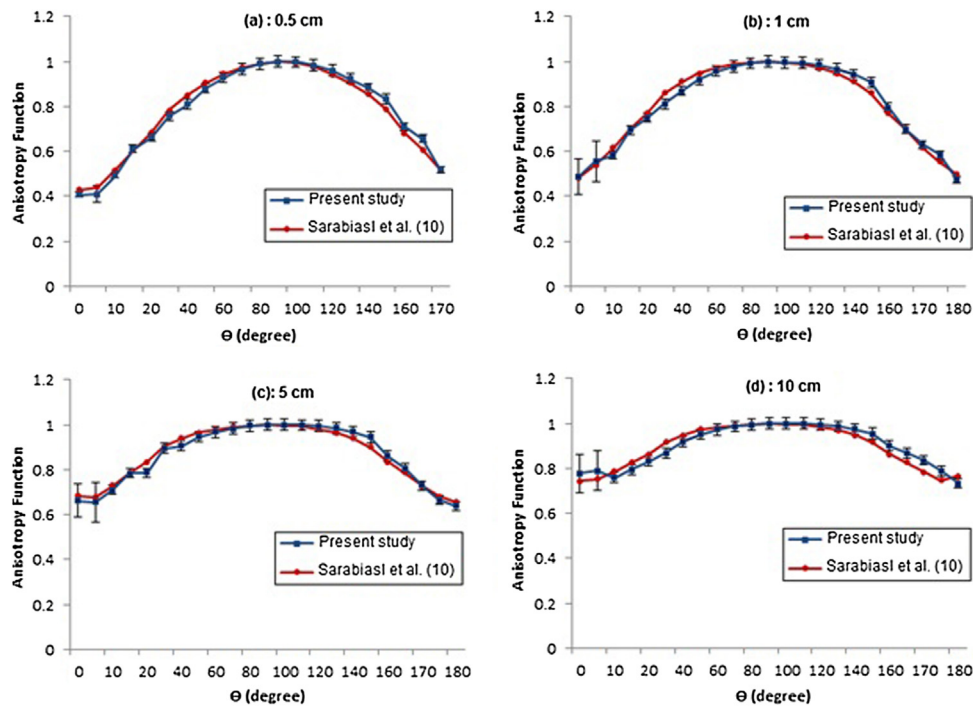


Fig. 3. The comparison of anisotropy function of the IRAsource source at distances of (a): 0.5 cm; (b): 1 cm; (c): 5 cm; and (d): 10 cm from the present study and Sarabiasl et al. study.<sup>10</sup>

the interaction of photons with phantom materials needed to be considered. For all brachytherapy models discussed in this study, <sup>192</sup>Ir source; an identical photon spectrum of the source and water phantom material were used. The important factors influencing the RDF of different <sup>192</sup>Ir brachytherapy models were the radius of active cores and the thicknesses of capsules containing active cores of sources. The RDF values of different <sup>192</sup>Ir brachytherapy source models had also been affected by geometric parameters. It should be noted that the comparison of the RDF of IRAsource <sup>192</sup>Ir source and other clinical models indicated their consistency.

There is a potential of performing experimental imaging, like the autoradiography method, for precise validation of the IRAsource source geometry. However, there was no access to the real source in the present study and the geometry was adopted from the study by Sarabiasl et al.<sup>10</sup> Additionally, it is a well-established method that the geometry of a source is extracted from other similar studies. Performing autoradiography examinations on this source can be a subject of further studies on this source.

In Fig. 3, a comparison of the AF at the distances of 0.5, 1, 5, and 10 cm was shown for the IRAsource model in this study and the one reported by Sarabiasl et al.<sup>10</sup> Due to similar geometries, the AFs were consistent for the distances of 0.5, 1, 5, and 10 cm (Fig. 3). The AF values of the IRAsource <sup>192</sup>Ir source at a distance of 5 cm derived in this study and other <sup>192</sup>Ir models were depicted in Fig. 4. According to Fig. 4, the AF values were almost similar for all models at the angles ranging from 50° to 150°. However; at the tip and the end of the sources ( $\theta < 50^\circ$  or  $\theta > 150^\circ$ ), the oblique filtration of sources was reported different for all source models due to different geometric parameters. The differences in oblique filtration also affected the AF, as shown in Fig. 4. Based on the AF of different models at a distance of 5 cm from the center of the active core (Fig. 4), the Varisource model had the best isotropy due to its different geometry with the most active length and the least active diameter.

Although two independent studies of Sarabiasl et al. and Ayoobian et al. are adequate for the source verification, the dosi-

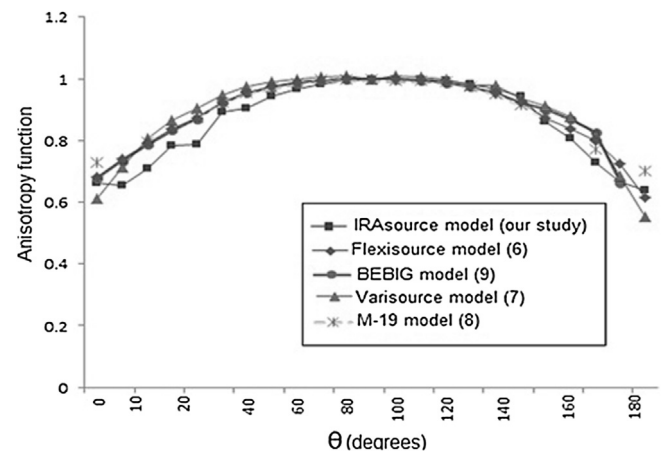


Fig. 4. Anisotropy function from this study and other investigators for <sup>192</sup>Ir HDR brachytherapy sources (IRAsource, Flexisource,<sup>6</sup> BEBIG,<sup>9</sup> Varisource VS2000,<sup>7</sup> M19<sup>8</sup>) at distance of 5 cm.

metric parameters of the IRAsource <sup>192</sup>Ir source determined in the present study can also be used for providing comprehensive dosimetric data or a brachytherapy database (like Carleton University<sup>23</sup> and European Society for Radiotherapy and Oncology (ESTRO) databases<sup>24</sup>) for this source model. The comprehensive data can be utilized for clinical applications as input data sets or validation of the treatment planning system used in brachytherapy via the IRAsource brachytherapy source.

## 5. Conclusion

In the present study, the IRAsource <sup>192</sup>Ir source model was simulated using a MC code to obtain the dosimetric parameters of this model according to TG-43 formalism. Comparing the results of this study with those of Sarabiasl et al. with regard to the IRAsource <sup>192</sup>Ir source model also suggested the acceptability of the source

simulation, which was only slightly different from the investigation by Sarabiasl et al. on this source. A comparison of the results of this study with different types of  $^{192}\text{Ir}$  brachytherapy sources also implied that the IRAsource source model for the DRC, RDF, and AF was analogous to previous data on various  $^{192}\text{Ir}$  sources, conventionally used in clinical contexts. However; small differences were observed between dosimetric parameters of these models, which could be due to different sizes of the source active parts and their capsules.

Consistent with the findings reported by Sarabiasl et al. and Ayoobian et al., the results of this study confirmed the application of IRAsource  $^{192}\text{Ir}$  source in clinical contexts.

### Funding

Cancer Research Center, Shahid Beheshti University of Medical Sciences.

### Conflict of interest

There is not any relationship that might lead to a conflict of interest.

### Acknowledgement

We would like to thank Cancer Research Center (Shahid Beheshti University of Medical Sciences) for financial support of this work

### References

1. Awan SB, Dini SA, Hussain M, et al. Cylindrical coordinate-based TG-43U1 parameters for dose calculation around elongated brachytherapy sources. *J Appl Clin Med Phys.* 2008;9(2):123–142.
2. Bahreyni Toossi MT, Ghorbani M, Rostami A, et al. Comparison of the hypothetical  $^{57}\text{Co}$  brachytherapy source with the  $^{192}\text{Ir}$  source. *Contemp Oncol.* 2016;20(4):327–334.
3. Perez-Calatayud BF, Das RK, DeWerd LA, et al. Dose calculation for photon-emitting brachytherapy sources with average energy higher than 50 keV: report of the AAPM and ESTRO. *Med Phys.* 2012;39(5):2904–2929.
4. Li Z, Das RK, DeWerd LA, et al. Dosimetric prerequisites for routine clinical use of photon emitting brachytherapy sources with average energy higher than 50 keV. *Med Phys.* 2007;34(1):37–40.
5. Rivard MJ, Coursey BM, DeWerd LA, et al. Update of AAPM task group No. 43 report: a revised AAPM protocol for brachytherapy dose calculations. *Med Phys.* 2004;31(3):633–674.
6. Granero D, Pérez-Calatayud J, Casal E, et al. A dosimetric study on the Ir-192 high dose rate flexisource. *Med Phys.* 2006;33(12):4578–4582.
7. Casado FJ, García-Pareja S, Cenizo E, et al. Dosimetric characterization of an  $^{192}\text{Ir}$  brachytherapy source with the Monte Carlo code PENELOPE. *Phys Med.* 2010;26(3):132–139.
8. Medich DC, Munro JJ. Monte Carlo characterization of the M-19 high dose rate Iridium-192 brachytherapy source. *Med Phys.* 2007;34(2):1999–2006.
9. Granero D, Perez-Calatayud J, Ballester F. Monte Carlo calculation of the TG-43 dosimetric parameters of a new BEBIG Ir-192 HDR source. *Radiother Oncol.* 2005;76(1):79–85.
10. Sarabiasl A, Ayoobian N, Jabbari I, et al. Monte Carlo dosimetry of the IRAsource high dose rate  $^{192}\text{Ir}$  brachytherapy source. *Australas Phys Eng Sci Med.* 2016;39(2):413–422.
11. Ayoobian N, Sarabiasl A, Poorbaygi H, et al. Gafchromic film dosimetry of a new HDR  $^{192}\text{Ir}$  brachytherapy source. *J Appl Clin Med Phys.* 2016;17(2):194–205.
12. Imaging and Radiation Oncology Core (IROC), Available at: [iroc.houston.mdanderson.org](http://iroc.houston.mdanderson.org), Accessed on: 11/11/2019.
13. Valencia University webpage. Dosimetry Parameters for source models used in Brachytherapy, Available at: [www.uv.es/braphyqs](http://www.uv.es/braphyqs), Accessed on: 11/11/2019.
14. Rivard M, Coursey B, DeWerd L, et al. Update of AAPM task group No. 43 report: a revised AAPM protocol for brachytherapy dose calculations. *Med Phys.* 2004;31(3):633–674.
15. National Nuclear Data Center. Nuclear data from NuDat, a web-based database maintained by the National Nuclear Data Center. Brookhaven National Laboratory, Upton, NY, USA. Available at: <http://www.nndc.bnl.gov/nudat2>. Accessed on: 25 Jan 2010.
16. Taylor R, Yegin G, Rogers D. Benchmarking BrachyDose: voxel based EGSnrc Monte Carlo calculations of TG-43 dosimetry parameters. *Med Phys.* 2007;34(2):445–457.
17. Taylor BN, Kuyatt CE. *Guidelines for Evaluating and Expressing the Uncertainty of NIST Measurement Results. NIST Technical Note 1297.* MD, USA: NIST; 1994.
18. Selvam TP, Sahoo S, Vishwakarma RS. EGSnrc-based Monte Carlo dosimetry of CSA1 and CSA2  $^{137}\text{Cs}$  brachytherapy source models. *Med Phys.* 2009;36(9):3870–3879.
19. Andreo P, Burns DT, Salvat F. On the uncertainties of photon mass energy-absorption coefficients and their ratios for radiation dosimetry. *Phys Med Biol.* 2012;57:2117–2136.
20. Rivard MJ, Granero D, Pérez-Calatayud J, Ballester F. Influence of photon energy spectra from brachytherapy sources on Monte Carlo simulations of kerma and dose rates in water and air. *Med Phys.* 2010;37:869–876.
21. Ballester F, Puchades V, Lluch JL, et al. Technical note: Monte-Carlo dosimetry of the HDR 12i and Plus  $^{192}\text{Ir}$  sources. *Med Phys.* 2001;28(12):2586–2591.
22. Granero D, Vijande J, Ballester F, et al. Dosimetry revisited for the HDR 192Ir brachytherapy source model mHDR-v2. *Med Phys.* 2011;38(1):487–494.
23. The CLRP TG-43 Parameter Database for Brachytherapy, Available at: <http://www.physics.carleton.ca/clrp/seed.database>. Accessed on: 22/9/2018.
24. European Society for Radiotherapy and Oncology, Available at: <https://www.estro.org/about/governance-organisation/committees-activities/tg43>. Accessed on: 22/9/2018.